BEAM TEST OF C-BAND COMPACT ACCELERATING STRUCTURE MADE OF LONGITUDINALLY-SPLIT TWO HALVES

M. Kimura†, H. Hara, K. Higa, N. Shigeoka, T. Sugano, S. Takagi
Mitsubishi Heavy Industries Machinery System, Ltd., Kobe, Japan
T. Abe, High Energy Accelerator Research Organization, Tsukuba, Ibaraki, Japan

Abstract

Our 6 MeV medical C-band accelerating structure uses a disk-stacked method, in which multiple oxygen-free copper components are stacked along the beam axis. Because the side-coupled (SC) re-entrant structure has a complex shape and many components, manufacturing efficiency is limited. In contrast, the longitudinally-split method divides the structure along a plane including the beam axis, typically into two halves or four quadrants, thereby reducing the number of components. Based on development experience of the quadrant-type X-band accelerating structures in the CLIC project, we have been developing a compact, high-gradient, high-shunt impedance SC-type C-band accelerating structure using this concept. In previous work, we reported fabrication of the full-scale structure, low-power RF test result, and preliminary first beam acceleration test limited by the available test facility. This paper reports recent progress, including RF conditioning and a high-power beam test under actual operating conditions.

INTRODUCTION

Background and Objectives

Compactness, high accelerating gradient, and improved manufacturability are increasingly required for medical and industrial electron accelerators. Our conventional 6 MeV SC-type C-band accelerating structure uses a disk-stacked method, which requires many parts and a complex brazing process.

A longitudinally-split concept, also called horizontal split, has been studied for high-gradient accelerating structures [1,2]. In this approach, the cavity is divided along a plane including the beam axis and machined as integrated halves, reducing part count and simplifying fabrication and assembly.

Based on this concept, we developed a longitudinally-split SC-type C-band accelerating structure to simplify fabrication and assembly while maintaining performance comparable to that of the conventional structure.

Overview of the SC-Type C-band Structure

Table 1 summarizes the main specifications, and Fig. 1 compares the conventional and longitudinally-split configurations.

The developed structure consists of a buncher section, accelerating cells, coupling cells, waveguide, and vacuum piping, with a total length of approximately 300 mm. To improve manufacturability while maintaining RF performance, the accelerating cells adopt a nose-cone geometry under a pending patent application (PCT/JP2023/023388). In addition, the coupling cells are arranged on one side of the beam axis to improve material utilization efficiency, compared with a layout in which they are placed on both sides.

The number of components was reduced from 59 in the conventional structure to 25 in the longitudinally-split structure, and the brazing process was simplified from a two-step to a one-step procedure.

Table 1: Outline of the SC-Type C-Band Structure

Item	Value
Frequency	5714±0.5 MHz
Coupling β	1.4 ~ 2.0
Beam energy	6 MeV
Beam current	> 75 mA
Beam Transmittance	> 40 %
Beam diameter	1.5 ~ 2.0 mm

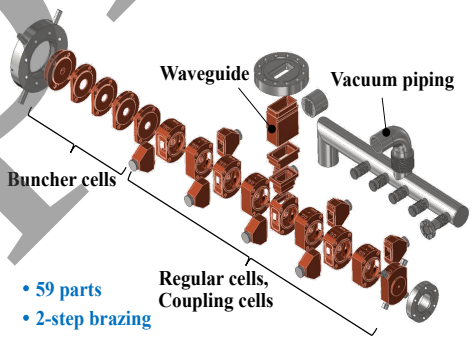

(a) Disk-stacked structure (conventional structure)

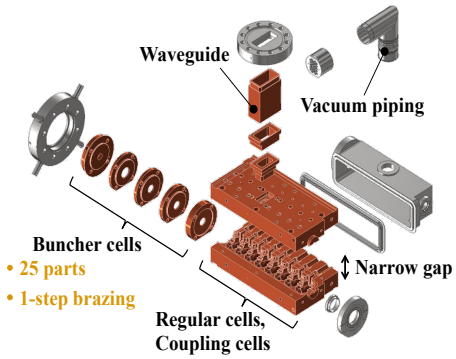

(b) Longitudinally-split method

Figure 1: Structural comparison of SC-type C-band accelerating structures.

† masashi.kimura.ck@mhi.com

FULL-SCALE PROTOTYPE

A full-scale prototype was fabricated for the beam tests under actual operating conditions. The prototype was assembled with a buncher, target, electron gun, RF window, vacuum components, and an ion pump. The design details of the full-scale prototype are described in [3,5], and its manufacturability evaluation is reported in [4].

The measured unloaded Q (Q_0) was 10006, in good agreement with the simulated value of 10087. The measured operating frequency was 5713.53 MHz, satisfying the target specification of 5714±0.5 MHz. Figure 2 shows the bead-pull measurement result. The measured electric-field profile also agreed well with the simulation, confirming that the full-scale prototype provided RF characteristics suitable for beam testing.

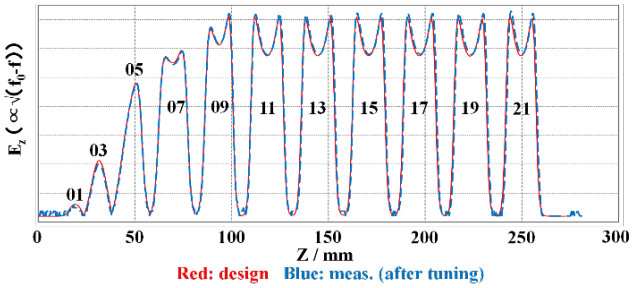

Figure 2: Bead-pull measurement result.

DEMONSTRATION TESTS IN THE ACTUAL OPERATING ENVIRONMENT

Beam Test Results

Figure 3 shows the configuration of the beam test system under actual operating conditions. An X-ray detector was placed 880 mm downstream of the target for dose-rate measurement. Additional beam tests were carried out, following the previous studies [6,7], using the currently available test facility to evaluate the full-scale longitudinally-split structure under the maximum achievable operating conditions.

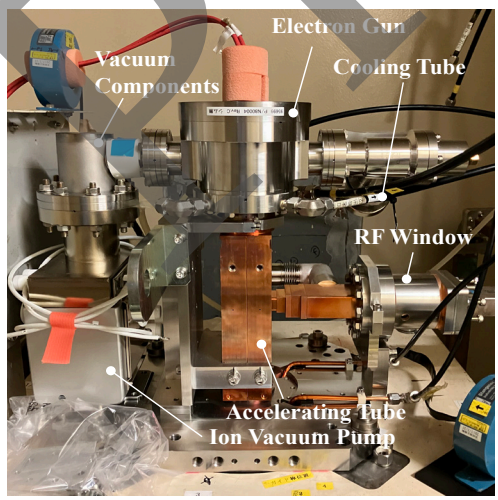

Figure 3: Beam test setup under actual operating conditions.

The measurement results are summarized in Table 2. In the present test, the input RF power reached approximately 2.8 MW at a pulse width of 4 μs and a repetition rate of 280 pps. Under these conditions, a gun current of 124 mA and a target current of 72 mA were obtained, corresponding to a beam transmission of 58.1%. In addition, the measured dose rate was 649.8 cGy/min, achieving the target value of 646 cGy/min. These results indicate that the full-scale prototype achieved beam acceleration performance comparable to the target values.

Table 2: Beam Test Results

Item	Test result	Target performance
Pulse width	4 μs	4 μs
Pulse repetition	280 pps	390 pps
Input RF power	Approx. 2.8 MW	Approx. 3 MW
Gun current	124 mA	120 mA
Target current	72 mA	75 mA
Transmission	58.1 %	> 40 %
Dose rate	649.8 cGy/min	646 cGy/min

Conditioning Histories

Figure 4 compares the RF conditioning histories of the longitudinally-split and conventional structures. The upper panel shows an expanded view of the low-pulse region, and the lower panel shows the higher-pulse region. To clarify the effect of the peak surface electric field, estimated normalized peak-field trends are also overlaid.

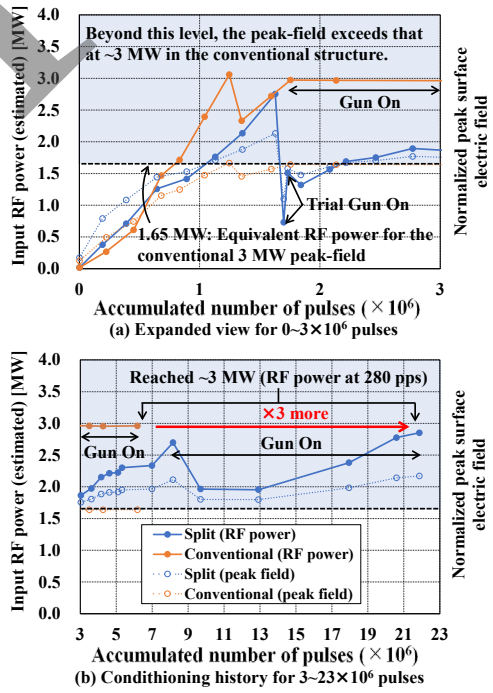

Figure 4: Comparison of RF conditioning histories of the conventional and longitudinally-split structures.

The difference remained small below the peak-field level corresponding to approximately 3 MW in the conventional structure. Above this level, the accumulated pulse count increased more rapidly for the split structure, and achieving approximately 3 MW required more than three times as many pulses. This indicates that the additional conditioning demand was concentrated in the high-field region.

Possible contributing factors to the prolonged conditioning process include the following:

- Higher peak surface electric field: The cavity shape was designed to maintain shunt impedance comparable to that of the conventional structure while ensuring manufacturability by machining. As a result, the peak surface electric field is approximately 35% higher than that of the conventional design.
- Rougher inner surfaces due to the different machining method: In the regular cells, the machining process was changed from ultra-precision turning to five-axis machining, which may produce rougher inner surfaces, enhance local electric fields, and increase the number of discharge events required for stabilization.
- Gas retention and local non-uniformity associated with narrow gaps along the split interface: These narrow gaps may create poorly pumped regions, and brazing filler flow into them may introduce local geometric non-uniformity.

Although these factors are possible contributors, the root cause of the prolonged conditioning process has not yet been identified.

INTERNAL INSPECTION

After the beam tests, internal inspection was carried out using a borescope. Because of the limited accessibility of the borescope, only a limited portion of the cavity interior could be observed. Figure 5 shows noteworthy observation by the borescope.

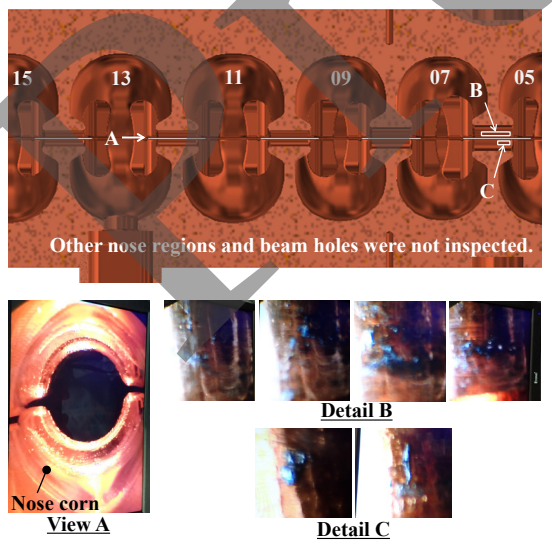

Figure 5: Noteworthy observation by the borescope.

In View A, multiple craters were observed on the nose region of Cell 13, which corresponds to a relatively high-field area in the field analysis. In Details B and C, a black trace, likely beam-related, was found in the beam hole between Cells 05 and 07.

At this stage, it is still unclear whether these observations are specific to the longitudinally-split structure or are influenced by the present test history and inspection limitations. Detailed investigation after sectioning is planned in order to identify the damage mechanisms and their relation to the prolonged conditioning process.

MANUFACTURING ADVANTAGES

Compared with the conventional disk-stacked structure, the longitudinally-split structure simplifies the overall fabrication and assembly flow by reducing the need for ultra-precision machining and enabling a simpler step-brazing process with fewer parts.

In the present prototype, the split design was applied only to the regular cells. Even in this limited configuration, the reduced part count simplified brazing and assembly. Further simplification is expected if the same concept is extended to the buncher cells.

Therefore, from a manufacturing viewpoint, the proposed structure offers clear advantages. However, a comprehensive evaluation should include not only the benefits in fabrication and assembly but also the burden associated with the prolonged conditioning process.

CONCLUSION AND FUTURE WORK

Conclusion

A longitudinally-split SC-type C-band accelerating structure was developed. Beam tests showed performance comparable to the nominal operation of a conventional 6 MeV-class structure. However, the split structure required more than three times the accumulated number of pulses to reach approximately 3 MW. Borescope inspection revealed internal features, although their relation to the split structure requires further analysis. The structure nevertheless showed clear manufacturing advantages.

Future Work

Future work will focus on detailed internal observation after sectioning, analysis of the cause of the prolonged RF conditioning, and feedback of the results into the design and fabrication process. In parallel, the relation between the observed internal features and the conditioning behavior will be further investigated.

ACKNOWLEDGMENTS

The authors would like to express their sincere gratitude to Drs. Higo and Higashi of KEK for their invaluable guidance and support throughout this development, including the loan of the borescope and valuable insight into the interpretation of the observed traces. The authors also thank Dr. Yoshida of KEK for providing the test stand for the high-power measurements.

REFERENCES

[1] M. Aicheler *et al*., "A multi-TeV linear collider based on CLIC technology: CLIC conceptual design report", CERN, Geneva, Switzerland, Rep. CERN-2012-007, 2012. doi:10.5170/CERN-2012-007

[2] T. Abe *et al*., "Fabrication of improved quadrant-type x-band high-gradient accelerating structure", in *Proc. PASJ'19*, Kyoto, Japan, Jul.-Aug. 2019, paper WEOH04, pp. 22-26.

[3] T. Abe *et al.*, "Design and test of c-band compact accelerating structure made of longitudinally-split two halves", in *Proc. PASJ'24*, Yamagata, Japan, Jul.-Aug. 2024, paper FROT05, pp. 151-155.

[4] M. Kimura *et al*., "Fabrication of c-band compact accelerating structure made of longitudinally-split two halves", in *Proc. PASJ'24*, Yamagata, Japan, Jul.-Aug. 2024, paper FRP042, pp. 955-958.

[5] T. Abe, "Longitudinally-split side-coupled high-shunt-impedance c-band structure fabricated in two halves" presented at HG'25, Merida, Yucatan, Mexico, Mar. 2025, unpublished.

[6] M. Kimura *et al*., "Development of c-band compact accelerating structure made of longitudinally-split two halves", in *Proc. IPAC'25*, Taipei, Taiwan, Jun. 2025, pp. 2377-2380. doi:10.18429/JACoW-IPAC2025-WEPS065

[7] M. Kimura *et al*., "Development of c-band compact accelerating structure made of longitudinally-split two halves", in *Proc. PASJ'25*, Tokyo, Japan, Aug. 2025, paper WEP060, pp. 368-371.